

Implications of LHC Searches for Massive Graviton

Yong Tang ^a

Physics Division, National Center for Theoretical Sciences, Hsinchu, Taiwan

(Dated: August 1, 2012)

Abstract

With the latest LHC available results, we consider the generic constraints on massive graviton. Both dijet and dilepton resonance searches are used. The limits on parameter space can be applied to many models. As an illustration, we show the constraints for Randall-Sundrum (RS) model. Implications on massive graviton and the coupling strength are discussed. For $k/M_{pl} = 0.1$, $M_G < 2.2$ TeV region is excluded at 95% confidence level. We also present some interesting implications on the RS radion with respect to the 125 GeV excess at the LHC. For $k/M_{pl} = 0.1$, $\Lambda_\phi < 13.8$ TeV is excluded where Λ_ϕ is the scale to characterize the interaction strength of radion.

^a ytang@phys.cts.nthu.edu.tw

I. INTRODUCTION

The standard model (SM) with gauge group $SU(3) \times SU(2) \times U(1)$ has been very successful in explanation for experimental results. Although the exact mechanism for electroweak symmetry breaking is still unclear, the recent hint of 125 GeV excess [1, 2] may suggest the higgs mechanism. Then the hierarchy problem in SM, electroweak breaking scale being so smaller than Planck scale, still exists and motivates new physical ideas. Among these ideas to solve the hierarchy problem, extra-dimension [3, 4] is one of the simplest ways.

Numerous models with extra-dimensions describing possible new physics beyond SM predict massive gravitons [5, 6]. The masses of these particles are usually at the TeV scale if these models were trying to solve the hierarchy problem. Then these massive gravitons can be produced at the large hadron collider (LHC). In some cases, the cross section is large enough so that exclusion limit or discovery can be reached for the considered models.

Extra-dimensional models have many phenomenological consequences [7–12]. Before LHC era, flavour physics and electroweak precision observables have already give some limits. In our study, we shall discuss the constraints from direct searches at the LHC. Other than specifying on a single model, we will study the general properties of massive graviton. The discussions and constraints are applicable to a wide class of models. As an illustration, we show the constraints for Randall-Sundrum (RS) model.

The paper is organized as follows. In section II, we introduce the general framework for later discussion and the necessary ingredients for searches or exclusions for massive graviton at the LHC. In section III, we use the latest CMS and ATLAS data to constrain the parameters for the lightest massive graviton. Both dijet and dilepton final states are considered. In section IV, we show that constraints has interesting implications in a specific and popular model, warped extra dimension. Finally, summary and conclusion are given.

II. GENERIC FRAMEWORK ON MASSIVE GRAVITON

Massive gravitons exist in various models usually with extra dimensions. The compactification of extra-dimensional leads to Kaluza-Klein towers of particle spectrums. The lowest states of these towers usually are the SM particles, and the higher states represent these new heavy particles. With exact mass depending on the details of models, massive Kaluza-Klein

particles are roughly at TeV scale if heirarchy problem is solved. Among them, massive gravitons serve as indispensible ingredients.

A. Interactions with SM

The field that describes a spin-2 particle is a tensor, $h_{\mu\nu}$. In a general effective theory with $h_{\mu\nu}$, all gauge invariant terms, both renormalizable and non-renormalizable, should be written down in the lagrangian. However, such a theory will have too many free parameters to be considered. Thus, in this paper, we should assume a minimal setup that massive graviton shall couple to standard model particles with universal form as same as the massless one, except with different strength and a non-zero mass. This universality is quite general as long as massive graviton is derived from the space-time metric.

For direct production at the LHC, we only need the lowest interaction term,

$$\mathcal{L}_{\text{int}} = -\frac{1}{M_{pl}} T^{\alpha\beta} h_{\alpha\beta}^{(0)} - \frac{1}{\Lambda_G} T^{\alpha\beta} h_{\alpha\beta}, \quad (2.1)$$

here and after, we will use $h_{\mu\nu}^0$ and $h_{\mu\nu}$ for massless and massive graviton, respectively. $T^{\alpha\beta}$ is the energy-momentum tensor of SM field. And the interactions between massive graviton and SM particle are solely determined by Λ_G . In general, there could be more than one massive graviton. For simplicity in this work, we will only concentrate on and refer to the lowest massive graviton, $h_{\mu\nu}$, if not stated explicitly. Early discussions on searches for massive gravitons are referred to [13–17].

B. Production at the LHC

Based on the interaction term, it is immediately realized that the topology for production of massive graviton is Drell-Yan like process. At the LHC with proton-proton collision, the two main channels to produce massive graviton are gluon-gluon fusion and quark-antiquark annihilation processes, Fig. (1). Vector boson fusion processes or other associated production are neglected for leading-order approximation throughout this work.

For hadronic collision, the total cross section is the convolution of the parton distribution functions (PDFs) with the partonic cross section,

$$\sigma = \int dx_1 dx_2 f_{q_1}(x_1, \mu_F) f_{q_2}(x_2, \mu_F) \hat{\sigma}(q_1 q_2 \rightarrow G^*; \hat{s}), \quad (2.2)$$

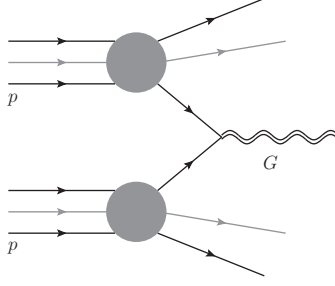


FIG. 1. Feynman diagram for the massive graviton production at the LHC. The produced gravitons then decay to SM particles.

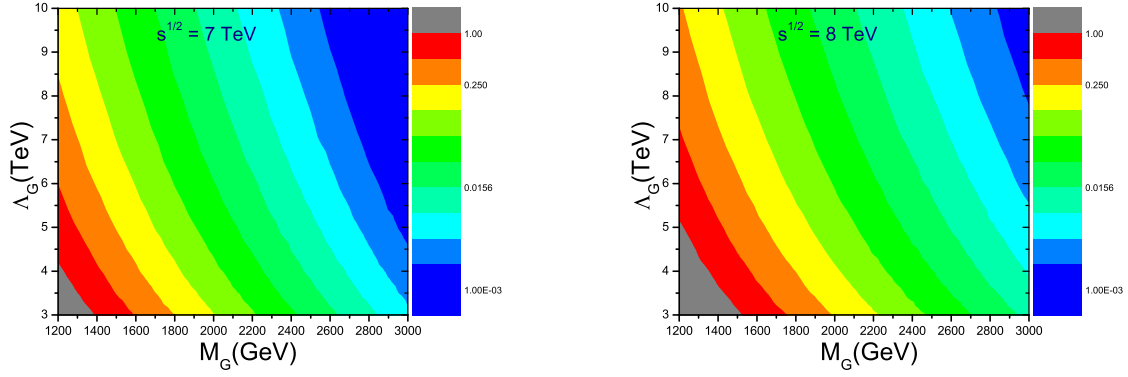


FIG. 2. Colorred map of cross section (pb) for massive graviton production at the LHC with $\sqrt{s} = 7$ TeV (left) and $\sqrt{s} = 8$ TeV (right), respectively.

where $f_q(x, \mu_F)$ is the PDF for a parton q (quark and gluon) with momentum fraction x at the factorization scale μ_F , $\hat{\sigma}$ is the partonic cross section with the initial two partons of momentum fraction x_1 and x_2 , respectively, and $\hat{s} = x_1 x_2 s$.

We use Madgraph 5 [18, 19] with $\mu_F = M_G$ and CTEQ6L1 [20] PDF set, and show in Fig. (2) colorred maps of cross section with function as mass M_G and the scale Λ_G at the LHC with both $\sqrt{s} = 7$ TeV (Left figure) and $\sqrt{s} = 8$ TeV. The cross section smaller than 1 fb is shown in blue region at the right top corners. These two figures roughly show the relations between cross section and parameters. Compared to the $\sqrt{s} = 7$ TeV case, the colored map for $\sqrt{s} = 8$ TeV is shifted towards larger Λ_G and M_G .

C. Decay width and branching ratio

For direct search or exclusion of the massive graviton, we need to know the branching ratio of its decay channels. If massive graviton lies in the TeV mass regions, its decay products, standard model particles, are then on-shell. So for leading order consideration we only include the two-body decay channels. The individual decay rate to two final SM particles is listed in the appendix. In Fig. 3, we show the branching ratios for the main

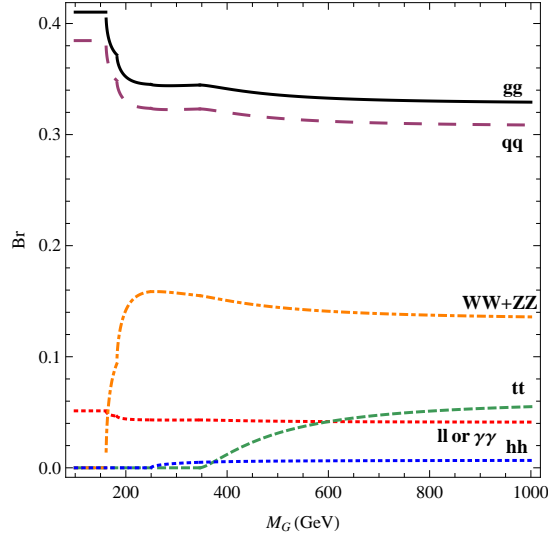


FIG. 3. Branching ratios, where $q = u, d, c, s, b$ and $l = e, \mu$. We have $Br(G \rightarrow ll) \simeq Br(G \rightarrow \Gamma\Gamma)$ as shown above.

decay channels. Here, we neglected the three-body decay with a off-shell W^* , Z^* or t at the low mass range. As shown in the figure, as the mass of graviton goes large compared with $2m_t$, branching ratios are almost fixed. Now it is easy to get the total decay width for large M_G ,

$$\Gamma_G \simeq \frac{M_G^3}{40\pi\Lambda_G^2} \left[(3+1) \times 6 \times \frac{1}{4} + (1 + \frac{1}{2}) \times \frac{13}{12} + (8+1) \times \frac{1}{2} + \frac{1}{12} \right] = \frac{293M_G^3}{960\pi\Lambda_G^2}.$$

In Table. I, we show branching ratios of the main decay channels for later use. The events at partonic level at the LHC then is proportional to $\sigma(pp \rightarrow G) \times Br(G \rightarrow ff)$ for narrow width approximation.

III. CONSTRAINTS FROM LHC DIRECT SEARCHES

The massive graviton couples to standard model particles through the energy-momentum tensor in the linear theory and the couplings are suppressed by a factor Λ_G . If the mass is at the TeV scale and the factor is not too large, then enough massive graviton can be produced at the LHC. Searches for the decay products of the graviton can be used to discover or constrain the parameter space of the model. Based on the final states, there are various search channels and if no excess is observed, each channel can give a constraint. In the section, we focus on the dijet and dilepton final states only.

A. Dijet Constraint

Dijets consist of quark jets and gluon jets. The shape of a gluon jet is wider than that of a quark one because gluon's effective coupling $C_A\alpha_S(C_A = 3)$ is larger than quark's $C_F\alpha_S(C_F = 4/3)$, then gluon jets are more likely to radiate. Modern detectors have the power to distinguish them. CMS [21] has presented limits for three kinds of dijet resonances, gluon-gluon, quark-quark(quark for q or \bar{q}) and gluon-quark. Because of the larger background from gluon jets, quark-quark dijet limit is the most stringent one among three . Then, we shall only consider the constraint from quark-quark dijet spectrum.

From the branching ratio in Table. I, we know that about 1/3 of the produced massive graviton will decay to quark-antiquark pairs ($q\bar{q}, q = u, d, s, c, b$). If the production rate is large, event distribution on dijet invariant mass m_{jj} shall show an additional peak at the graviton mass in the smooth QCD dijet background. If no excess is observed, constraints can be put on production rate using statistics(see appendix). So far, the latest published model-independent result on resonance search by dijet search is from CMS with 1 fb^{-1} [21]. Since no excess is observed yet, we shall use this result to constrain our parameter space.

The analysis of event samples in [21] relies on the following selection rules,

$$p_T > 10 \text{ GeV}, |\eta| < 2.5, |\Delta\eta| < 2.5 \text{ and } m_{jj} > 838 \text{ GeV}, \quad (3.1)$$

TABLE I. Branching ratio for the massive graviton to SM particle with $l = e, \mu$ and $q = u, d, s, c, b$.

channels	HH	gg	$\gamma\gamma$	W^+W^-	ZZ	$t\bar{t}$	$q\bar{q}$	l^+l^-
Br	2/293	96/293	12/293	24/293	12/293	16/293	90/293	12/293

where the definitions are

$$m_{jj} \equiv \sqrt{(E_1 + E_2)^2 - (\vec{p}_1 + \vec{p}_2)^2}, \quad p_T \equiv \sqrt{p_x^2 + p_y^2} = p \sin \theta,$$

$$\eta \equiv -\ln \tan \frac{\theta}{2}, \quad \Delta\eta = \eta_1 - \eta_2.$$

The renormalization scale is set to $\mu = p_T$ and CTEQ6L1 parton distribution functions [20] are used. A K-factor of 1.33 was used in [21].

For mass graviton, the signal acceptance A is about 0.72 for the events selected that satisfying the above kinematics requirements. This factor is nearly constant for large mass of G . Without seeing any excess of dijet mass spectrum, an upper limit at the 95% confidence level is obtained for $\sigma \times Br \times A$, the products of cross section, branching ratio and events acceptance. Since both Br and A are known, the limit then is translated to constraint on the Λ_G and M_G .

In Fig. 4, we show the limit as a solid line on the cross section contour of Λ_G and M_G . Regions at the left-handed side of the line is excluded at 95% confidence level. As is displayed in the figure, for M_G less than 1 TeV, Λ_G has to be larger than 2.5 TeV. As the mass get smaller, Λ_G needs to larger to accomodate. This is reasonable and intuitive otherwise we shall have seen a resonance around M_G .

B. Dilepton Constraint

The dilepton searches are involved with dielectron and dimuon final states where the main SM background is from Z/γ^* decay. For massive graviton, although the branching ratio to dilepton ($l = e, \mu$) is much smaller than that of dijet (7.5 times smaller exactly), the constraint or discovery potential is better due to the well-known and lower background.

The event selection follows [22] where for dielectron

$$E_T \equiv \sqrt{p_T^2 + m^2} > 25 \text{ GeV}, \quad |\eta| < 2.47 \text{ with excluding } 1.37 < |\eta| < 1.52, \quad (3.2)$$

and for dimuon $p_T > 25 \text{ GeV}$. The renormalization scale is set to $\mu = \sqrt{\hat{s}}$, the K-factor for dilepton final state varies between 1.6 to 1.8, depending on the graviton mass and Λ_G . In practice, 1.75 is used for $M_G > 750 \text{ GeV}$ [22]. With these kinematic requirements, the total signal acceptance A is 72% for dielectron and 47% for dimuon.

As shown in Fig. 4 as the dot-dashed line, the dilepton final state can give more stringent constraint due to both larger luminosity and better discriminating power, compared with

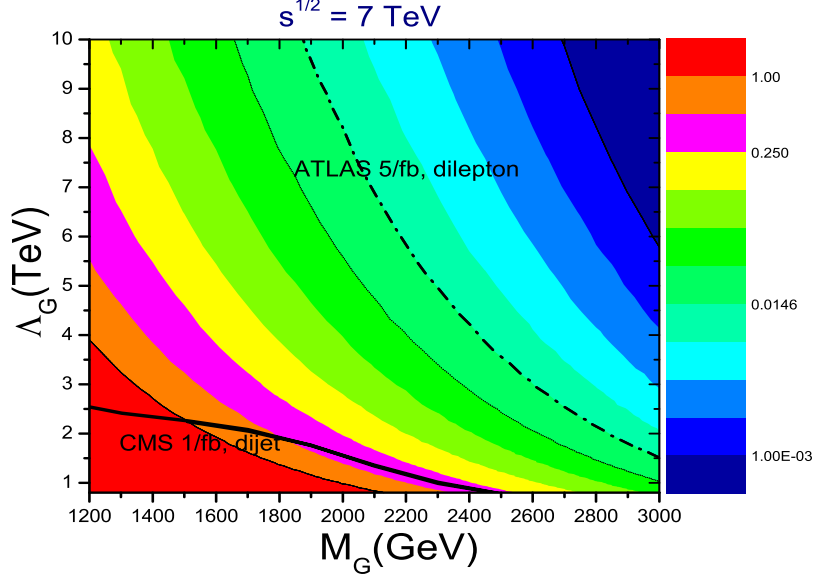


FIG. 4. No observation of dijet and dilepton event excess can put constraints on the parameters. Cross section is in pb. The solid line indicates the constraints from CMS with 1 fb^{-1} data [21] and the dot-dashed line shows the limit put by ATLAS with 5 fb^{-1} [22].

dijet limit with only 1 fb data. The limit on cross section is almost constant 2 TeV and 3 TeV because the constraint mainly comes from the observed event 4 in a single bin $[1200, 3000] \text{ GeV}$ of [22].

IV. CONSTRAINT ON WARPED EXTRA DIMENSION

A. Theory Overview

One of the most popular extra-dimensional models is Randall-Sundrum model. The physics behind RS model lies in the following geometry for the warped space-time [4],

$$ds^2 = e^{-2kT(x)|\varphi|} [\eta_{\mu\nu} + G_{\mu\nu}(x)] dx^\mu dx^\nu + T^2(x) d\varphi^2, \quad (4.1)$$

where $T(x)$ is referred to as the modulus field, $G_{\mu\nu}(x)$ as graviton and k is a scale of the order of the (reduced) Planck scale M_{pl} . To explain the hierarchy problem, the compactification radius or the vacuum expectation value (vev) of the modulus field, $r_c \equiv \langle T(x) \rangle$, is required to satisfy the relation $kr_c \sim 12$.

The action that determines the above geometry is

$$S = -M_*^3 \int d^5x \sqrt{g} R^{(5)}, \quad (4.2)$$

where the 5D reduced Planck scale M_* is related with the 4D (reduced) Planck scale M_{pl} ,

$$M_{pl}^2 = M_*^3 \int_{y=-r_c\pi}^{y=r_c\pi} e^{-2k|y|} dy = \frac{M_*^3}{k} (1 - e^{-2kr_c\pi}). \quad (4.3)$$

In the original RS model, SM particles are confined to the brane and only graviton can propagate in the bulk. Then a massive Kaluza-Klein graviton tower exists besides the massless graviton,

$$M_G^{(n)} = kx_n e^{-kr_c\pi} = x_n \frac{k}{M_{pl}} \Lambda_G, \quad \Lambda_G = M_{pl} e^{-kr_c\pi}, \quad J_1(x_n) = 0, \quad (4.4)$$

where J_1 is the Bessel function, and $x_1 \simeq 3.8317$, $x_2 \simeq 7.02$, $x_3 \simeq 10.17$, and $x_4 \simeq 13.32$. We shall only consider the effect of the lowest state $M_G \equiv M_G^1$. Both massless and massive gravitons can couple to standard model particles,

$$\mathcal{L} = -\frac{1}{M_{pl}} T^{\alpha\beta} h_{\alpha\beta}^{(0)} - \frac{1}{\Lambda_G} T^{\alpha\beta} \Sigma_{n=1}^{\infty} h_{\alpha\beta}^{(n)}. \quad (4.5)$$

$M_G = x_1 \frac{k}{M_{pl}} \Lambda_G$ implies that the larger M_G is, the larger ratio k/M_{pl} for fixed Λ_G .

Using the relation between the scale Λ_G and the mass M_G , we have the decay width for massive graviton in RS model,

$$\Gamma_G \simeq \frac{293M_G^3}{960\pi\Lambda_G^2} = \frac{293x_1^2 M_G}{960\pi} \left(\frac{k}{M_{pl}} \right)^2 \simeq 1.425 M_G \left(\frac{k}{M_{pl}} \right)^2. \quad (4.6)$$

In the RS original paper, $\frac{k}{M_{pl}}$ was assumed to be less than 1. Most discussions lie in $0.01 \leq \frac{k}{M_{pl}} \leq 1$ for theoretical and experimental studys. The estimation goes as follows. The 5D curvature scalar is $R_5 = -20k^2$, and requiring $|R| \simeq M_*^2$ with Eq. 4.3 gives

$$20k^2 \simeq (kM_{pl}^2)^{\frac{2}{3}} \implies \frac{k}{M_{pl}} \simeq \left(\frac{1}{20} \right)^{\frac{3}{4}} \simeq 0.1.$$

However, it was argued in [23, 24, 33] that R_5 should be compared with Λ^2 ($\Lambda \equiv 24^{1/3} \pi M_*$ is the energy scale at which the 5D gravity theory becomes strongly coupled), giving

$$20k^2 < \Lambda^2 \implies \frac{k}{M_{pl}} < \left(24^{2/3} \pi^2 \times \frac{1}{20} \right)^{\frac{3}{4}} \sim 2.88.$$

When k/M_{pl} is large, the decay width in Eq. 4.6 shows that it can be comparable with or even large than its mass. This can happen for strong interaction. For example, in PDG [25] $m_{f_0(600)} = (400 - 1200)$ MeV, but its width is in the range, $\Gamma = (600 - 1000)$ MeV. And $m_{\rho(770)} = 775.49$ MeV with width $\Gamma = 149.1$ MeV [26]. The finite decay width effect will be considered in the following section.

B. Limits on RS graviton

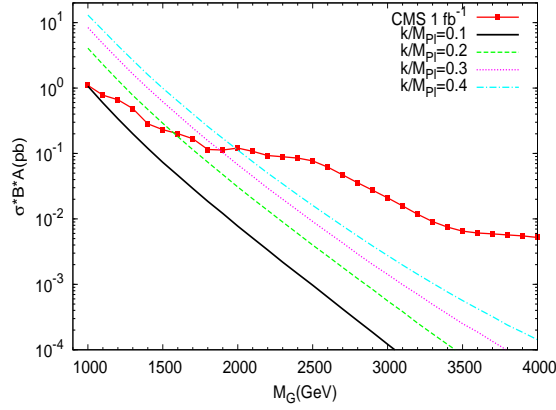


FIG. 5. Constraint on the parameters M_G and Λ_G with dijet events at CMS 1 fb [21].

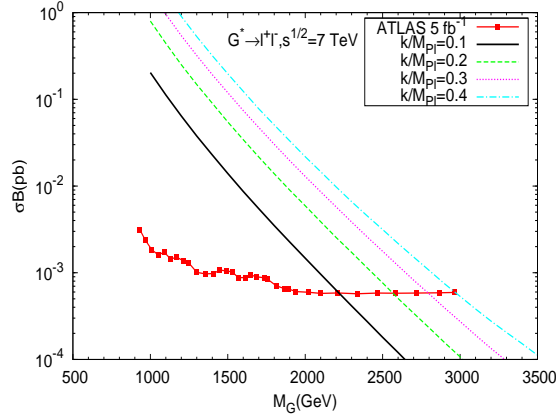


FIG. 6. Constraint on the parameters with dilepton events M_G and Λ_G , for various k/M_{pl} . The box points are extracted from [22].

For the lightest massive graviton in RS model, we have the relation Eq. 4.4, $M_G = x_1 \frac{k}{M_{pl}} \Lambda_G$. This feature shows that for fixed M_G , k/M_{pl} can effectively describe the interaction strength. Larger k/M_{pl} means smaller Λ_G and then stronger interaction. Both Tevatron and LHC has set some exclusion limit for $0.01 \leq \frac{k}{M_{pl}} \leq 0.1$. From the latest dilepton search result [22], the $k/M_{pl} = 0.1$ gives $M_G > 2.16$ TeV, implying $\Lambda_G > 5.64$ TeV.

In the following discussion, we shall extend the limit to $k/M_{pl} \geq 0.1$ region. As shown in Fig. 5 and 6, both the dijet and dilepton exclusion limits depend on the k/M_{pl} . In the dijet case, $M_G \leq 1$ TeV is excluded for $k/M_{pl} = 0.1$ and the limit turns higher mass for larger

k/M_{pl} . In the dilepton figure, $M_G \leq 2.2$ TeV is excluded for $k/M_{pl} = 0.1$, and again larger k/M_{pl} gives even more stringent constraints.

For Drell-Yan like s-channel production followed by immediate decay, there is a propagator of Breit-Wigner like

$$\frac{1}{\hat{s} - M_G^2 + iM_G\Gamma_G},$$

where the width of the massive particle Γ_G has been included. Usually, the width is very small for weak interactions, the narrow width approximation can be used and the final cross section is product of cross section for massive particle and branching ratio to final states. For large decay width, the above full Breit-Wigner propagator is needed.

How the events are distributed with respect to the m_{ll} depends on PDFs $f_q(x, \mu_F)$, M_G and k/M_{pl} . In the Fig. 7, we show several cases with different M_G and k/M_{pl} . When $k/M_{pl} < 0.3$, a clear resonance is still visible due to $\Gamma_G \leq 0.2M_G$ for $k/M_{pl} \leq 0.38$. When k/M_{pl} is large, the decay width goes large and the resonance get broadened.

The limits are shown in Fig. 8. For $M_G > 3.5$ TeV, the constraint is allmost fixed for large k/M_{pl} . This is simply due to k/M_{pl} cancellation between the coupling and decay width. And the processes can be described by a four-fermion contact interaction.

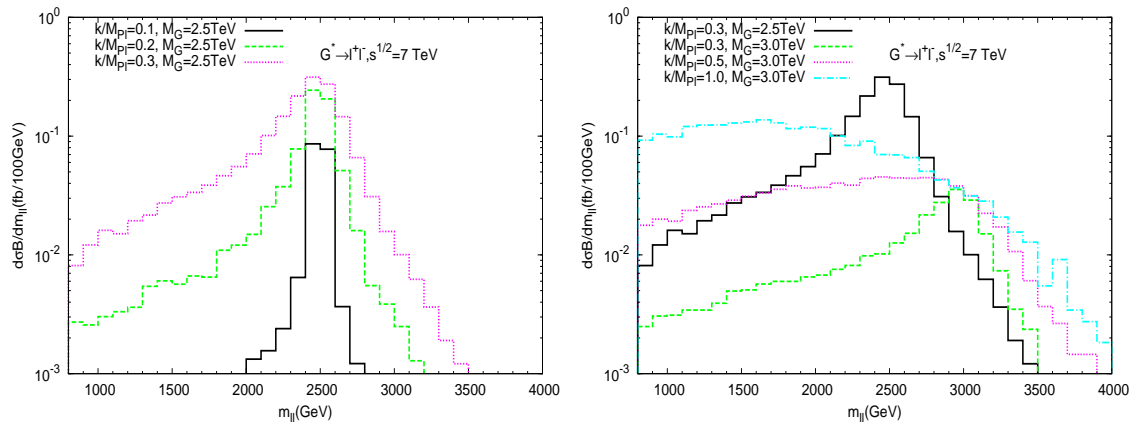


FIG. 7. Differential cross section as distributions with invariant mass m_{jj} . Two cases with $M_G = 2.5$ TeV(left) and $M_G = 3$ TeV(right) are shown.

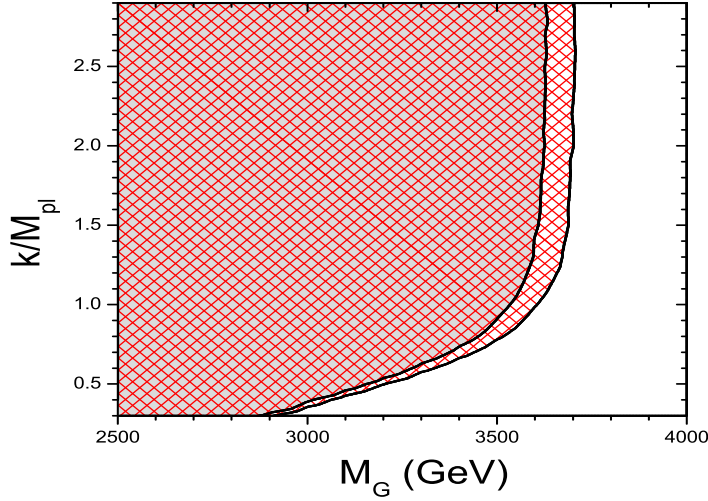


FIG. 8. Conservative limit on k/M_{pl} and M_G , where the shadowed region is excluded at least at 95% confidence level and the region between two solid lines indicates the effect of 10% uncertainty.

C. Implications for RS Radion

Randall-Sundrum scenario [4] is proposed to solve the hierarchy problem of the standard model. In the original version, no mechanism for dynamical origin of the $kr_c\pi$ is provided. Later, Goldberger and Wise [27, 28] introduced a mechanism to provide a potential for radion to stabilize the extra dimension. The radion, identified as the gravitational degree of freedom responsible for the fluctuations of the distance between branes, couples with standard model particles with similarity of higgs boson [29–31], except that couplings with massless gauge bosons could be larger.

The indications of 125 GeV excess at the LHC has intrigued many interesting discussions related with radion [32–37]. As shown in [32], the excess observed at the LHC can be explained by a 125 GeV RS radion with $\sigma(H)Br(H \rightarrow \gamma\gamma)/\sigma Br_{SM} \sim 2.1$ and smaller values for other channels relative to the corresponding ones in SM. Further phenomenological discussions are showed in [33–37].

The radion ϕ couples to SM particles [27, 28] as

$$\mathcal{L}_{int} = \frac{\phi}{\Lambda_\phi} T^\mu{}_\mu,$$

where $T_{\mu\nu}$ is energy-momentum tensor for SM particles and $\Lambda_\phi = \sqrt{6}M_{pl}e^{-kr_c\pi}$. Thanks to

the trace anomaly, this model leads to a larger branching ratio for $\phi \rightarrow gg$ or $\gamma\gamma$, relative to $h_{\text{SM}} \rightarrow gg$ or $\gamma\gamma$ in SM.

In this section, we show that the results of LHC searches for massive graviton have several interesting implications for the radion sector in RS model. The first and lightest massive Kaluza-Klein(KK) mode of $G_{\mu\nu}$ will couple to SM particles as $\mathcal{L}_{\text{int}} = -\frac{1}{\Lambda_G} h_{\mu\nu} T^{\mu\nu}$. As is shown above, the couplings of the massive graviton with SM particles are proportional to $1/\Lambda_G$ or $x_1 k/M_{pl}$ for a fixed M_G . Limits put on M_G for specified k/M_{pl} can then be translated to limits on Λ_G , therefore constraints on Λ_ϕ due to the relation $\Lambda_\phi = \sqrt{6}\Lambda_G$.

Using dijet final states from CMS [21] with 1 fb^{-1} data, we can exclude a RS graviton mass below 1 TeV for $k/M_{pl} = 0.1$ in Fig. 5. A straightforward calculation gives $\Lambda_\phi = \frac{\sqrt{6}}{x_1 k/M_{pl}} M_G = 6.4 \text{ TeV}$. With dilepton final states from ATLAS [22] with 5 fb^{-1} , we show in Fig. 6 that a RS graviton mass below 2.2 TeV is excluded at 95% confidence level with $k/M_{pl} = 0.1$, then the corresponding $\Lambda_\phi \simeq 13.8 \text{ TeV}$.

A smaller value of Λ_ϕ then requires a larger k/M_{pl} , although the latter of order 0.1 or less is preferred theoretically [7]. However, a larger k/M_{pl} means a more stringent constraint on M_G because the cross section for the graviton's production at the LHC is proportional to $(k/M_{pl})^2$. As shown in Fig. 8, when $k/M_{pl} = 0.3$, the limit for M_G is 2.8 TeV, then we have $\Lambda_\phi = 5.97 \text{ TeV}$. A limit of $M_G = 3.5 \text{ TeV}$ will give $\Lambda_\phi = 2.24 \text{ TeV}$ for $k/M_{pl} \simeq 1$. Even the largest but highly theoretically disfavoured $k/M_{pl} \simeq 2.88$ results in $\Lambda_\phi = 0.8 \text{ TeV}$ and $\sigma(H)Br(H \rightarrow \gamma\gamma)/\sigma Br_{\text{SM}} \sim 1.5$.

V. SUMMARY

In this work, we discuss the constraints on massive graviton with the latest LHC data. In a general framework, we show both dijet and dilepton limits on the two parameters, the mass M_G and coupling strength Λ_G . The limits are applicable to a wide class of models. As an illustration, we discuss the implications for RS massive graviton. For $k/M_{pl} = 0.1$, the dilepton search at ATLAS with 5 fb^{-1} excluded $M_G < 2.2 \text{ TeV}$ regions. The constraint becomes more stringent for larger k/M_{pl} .

As a byproduct, we show in RS model that constraints on massive graviton can give interesting implications on the radion sector. For $k/M_{pl} = 0.1$, the dijet search at CMS with 1 fb^{-1} excluded $\lambda_\phi < 6.4 \text{ TeV}$ intervals. And the dilepton search at ATLAS with 5 fb^{-1} can

exclude $\lambda_\phi < 13.8$ TeV regions. For $k/M_{pl} \simeq 1$, the low limit get relaxed to $\lambda_\phi \simeq 2.24$ TeV. These limits have a direct impact on the cross section $\sigma(pp \rightarrow \phi)$ of radion production at the LHC since $\sigma(pp \rightarrow \phi) \propto 1/\Lambda_\phi^2$.

ACKNOWLEDGMENTS

The author would like to thank Prof. H. Y. Cheng, K. Cheung, K. Hagiwara, and C. Q. Geng for helpful conversations. This work is supported by National Center for Theoretical Sciences, Hsinchu.

VI. APPENDIX

A. Decay rate

This subsection lists the decay rates for graviton to two standard model particles. The complete descriptions and full Feynman rules are referred to [5, 6]. The decay rate to two fermions, $G \rightarrow f\bar{f}$, is

$$\Gamma(G \rightarrow f\bar{f}) = N_c \frac{M_G^3}{160\pi\Lambda_G^2} (1 - 4x_f)^{\frac{3}{2}} \left(1 + \frac{8}{3}x_f\right),$$

where N_c is equal to 3 for quarks and 1 for leptons. For vector weak bosons final states, the rate is

$$\Gamma(G \rightarrow WW/ZZ) = \delta \frac{M_G^3}{40\pi\Lambda_G^2} (1 - 4x_V)^{\frac{1}{2}} \left(\frac{13}{12} + \frac{14}{3}x_V + 4x_V^2\right),$$

where $\delta = 1(\frac{1}{2})$ for $W(Z)$, respectively. For the massless final states, gluon and photon, we have

$$\Gamma(G \rightarrow gg/\gamma\gamma) = N_G \frac{M_G^3}{80\pi\Lambda_G^2}.$$

Here $N_G = 1(8)$ for $\gamma(g)$. Finally, the decay rate to higgs bosons is

$$\Gamma(G \rightarrow HH) = \frac{M_G^3}{480\pi\Lambda_G^2} (1 - 4x_H)^{\frac{1}{2}}.$$

In all the above formulas, $x_i = m_i^2/M_G^2, i = f, V, H$.

B. Bayesian inference

In this subsection, we briefly outline the statistics used in the context. Based on Bayesian inference, given the data or events observed, one can estimate the probability density of the parameter s (the signal or cross section, for example) predicted by a theoretical model,

$$p(s|\text{data}) = \frac{\mathcal{L}(\text{data}|s)\pi(s)}{\mathcal{N}},$$

$p(s|\text{data})$ is the posterior probability density function (PDF), $\mathcal{L}(\text{data}|b, s)$ is the likelihood function, $\pi(s)$ is the prior PDF, and \mathcal{N} is the normalization constant,

$$\mathcal{N} = p(\text{data}|s) = \int \mathcal{L}(\text{data}|s) ds.$$

Upper limit x can be put on s with 95% confidence level when

$$\int_0^x p(s|\text{data}) ds = 0.95.$$

In a counting experiment, events are the sum of background and signal, the likelihood function is actually $\mathcal{L}(\text{data}|b, s)$ which is given by

$$\mathcal{L}(\text{data}|b, s) = \text{Poisson}(d|b, s) = \frac{(b + s)^d}{d!} e^{-(b+s)},$$

where d is the number of the observed events, b and s are predicted by theory for background and signal, respectively. For example, when $d = 2$, $b = 0.92$, then the above formalism gives the upper limit with 95% confidence level $s \leq x = 5.45$. Since s is proportional to the cross section which is a function of the parameters in the model. Then limit set on s can be translated to the parameters.

For data collected into N bins, the above formulas can be generalized to

$$\mathcal{L}(\text{data}|b, s) = \prod_{i=1}^N \text{Poisson}(d_i|b_i, s_i) = \prod_{i=1}^N \frac{(b_i + s_i)^{d_i}}{d_i!} e^{-(b_i+s_i)},$$

where d_i, b_i, s_i corresponds to the quantities in the i -th bin. Details and examples can be found in [38] where uncertainty effect is also discussed.

[1] G. Aad *et al.* [ATLAS Collaboration], Phys. Lett. B **710**, 49 (2012) [arXiv:1202.1408 [hep-ex]].

- [2] S. Chatrchyan *et al.* [CMS Collaboration], arXiv:1202.1488 [hep-ex].
- [3] N. Arkani-Hamed, S. Dimopoulos and G. R. Dvali, Phys. Lett. B **429**, 263 (1998) [hep-ph/9803315].
- [4] L. Randall and R. Sundrum, Phys. Rev. Lett. **83**, 3370 (1999) [hep-ph/9905221].
- [5] G. F. Giudice, R. Rattazzi and J. D. Wells, Nucl. Phys. B **544**, 3 (1999) [hep-ph/9811291].
- [6] T. Han, J. D. Lykken and R. -J. Zhang, Phys. Rev. D **59**, 105006 (1999) [hep-ph/9811350].
- [7] H. Davoudiasl, J. L. Hewett and T. G. Rizzo, Phys. Rev. D **63**, 075004 (2001) [hep-ph/0006041].
- [8] C. Csaki, M. L. Graesser and G. D. Kribs, Phys. Rev. D **63**, 065002 (2001) [hep-th/0008151].
- [9] J. F. Gunion, M. Toharia and J. D. Wells, Phys. Lett. B **585**, 295 (2004) [hep-ph/0311219].
- [10] M. S. Carena, E. Ponton, J. Santiago and C. E. M. Wagner, Phys. Rev. D **76**, 035006 (2007) [hep-ph/0701055].
- [11] C. Csaki, A. Falkowski and A. Weiler, JHEP **0809**, 008 (2008) [arXiv:0804.1954 [hep-ph]].
- [12] S. Casagrande, F. Goertz, U. Haisch, M. Neubert and T. Pfoh, JHEP **0810**, 094 (2008) [arXiv:0807.4937 [hep-ph]].
- [13] I. Antoniadis, K. Benakli and M. Quiros, Phys. Lett. B **460**, 176 (1999) [hep-ph/9905311].
- [14] H. Davoudiasl, J. L. Hewett and T. G. Rizzo, Phys. Rev. Lett. **84**, 2080 (2000) [hep-ph/9909255].
- [15] E. Accomando, I. Antoniadis and K. Benakli, Nucl. Phys. B **579**, 3 (2000) [hep-ph/9912287].
- [16] J. Bijnens, P. Eerola, M. Maul, A. Mansson and T. Sjostrand, Phys. Lett. B **503**, 341 (2001) [hep-ph/0101316].
- [17] B. C. Allanach, K. Odagiri, M. A. Parker and B. R. Webber, JHEP **0009**, 019 (2000) [hep-ph/0006114].
- [18] J. Alwall, M. Herquet, F. Maltoni, O. Mattelaer and T. Stelzer, JHEP **1106**, 128 (2011) [arXiv:1106.0522 [hep-ph]].
- [19] K. Hagiwara, J. Kanzaki, Q. Li and K. Mawatari, Eur. Phys. J. C **56**, 435 (2008) [arXiv:0805.2554 [hep-ph]].
- [20] J. Pumplin, D. R. Stump, J. Huston, H. L. Lai, P. M. Nadolsky and W. K. Tung, JHEP **0207**, 012 (2002) [hep-ph/0201195].
- [21] CMS Collaboration, Phys. Lett. B **704**(2011)134.
- [22] The ATLAS Collaboration, ATLAS-CONF-2012-007.

- [23] Z. Chacko, M.A. Luty, and E. Ponton, J. High. Energy.Phys. 07(2000) 036.
- [24] K. Agashe, H. Davoudiasl, G. Perez and A. Soni, Phys. Rev. D **76**, 036006 (2007).
- [25] K. Nakamura *et al.* [Particle Data Group Collaboration], J. Phys. G **37**, 075021 (2010).
- [26] Thanks to Prof. H. Y. Cheng for pointing out these.
- [27] W. D. Goldberger and M. B. Wise, Phys. Rev. Lett. **83** (1999) 4922 [hep-ph/9907447].
- [28] W. D. Goldberger and M. B. Wise, Phys. Lett. B **475** (2000) 275 [hep-ph/9911457].
- [29] V. Barger and M. Ishida, Phys. Lett. B **709**, 185 (2012) [arXiv:1110.6452 [hep-ph]].
- [30] H. de Sandes and R. Rosenfeld, Phys. Rev. D **85**, 053003 (2012) [arXiv:1111.2006 [hep-ph]].
- [31] V. Barger, M. Ishida and W. -Y. Keung, Phys. Rev. Lett. **108**, 101802 (2012) [arXiv:1111.4473 [hep-ph]].
- [32] K. Cheung and T. -C. Yuan, Phys. Rev. Lett. 108, **141602** (2012) [arXiv:1112.4146 [hep-ph]].
- [33] B. Grzadkowski, J. F. Gunion and M. Toharia, Phys. Lett. B **712**, 70 (2012) [arXiv:1202.5017 [hep-ph]].
- [34] M. Frank, B. Korutlu and M. Toharia, arXiv:1204.5944 [hep-ph].
- [35] Y. Tang, arXiv:1204.6145 [hep-ph].
- [36] H. Davoudiasl, T. McElmurry and A. Soni, arXiv:1206.4062 [hep-ph].
- [37] J. Chang, K. Cheung, P. -Y. Tseng and T. -C. Yuan, arXiv:1206.5853 [hep-ph].
- [38] G. Choudalakis, arXiv:1110.5295 [hep-ph].